Title

Hygrothermal recovery of compression wood in relation to elastic growth stress and its physicochemical characteristics

Authors

Miyuki U Matsuo[1]*, Ginji Niimi[1], K.C. Sujan[1], Masato Yoshida[1], Hiroyuki Yamamoto[1]

Affiliation

[1]Graduate School of Bioagricultural Sciences, Nagoya University

Address

[1]Furo-cho, Chikusa-ku, Nagoya 464-8601, Japan

****Corresponding author***

Miyuki (Ueda) Matsuo

Telephone: +81-52-789-4151

Fax: +81-52-789-4150

E-mail: miyuki@agr.nagoya-u.ac.jp

Abstract

Hygrothermal recovery (HTR), the dimensional changes in wood induced by hygrothermal treatment, was investigated by using both compression and normal wood of sugi (*Cryptomeria japonica*). The elastic released strain of growth stress was measured on living tree surfaces; subsequently, the specimens were taken from the same position to measure HTR. HTR was measured as dimensional changes due to treatment at 20, 40, 60, 80, and 100°C in hot water ranging from 200 minutes to 177 days. The intensity of HTR had a positive relationship with elastic released strain of growth stress. This result suggests that HTR is the relaxation of the viscoelastic component of growth stress accumulated during the maturation process of trees. The rate of HTR clearly showed a time-temperature dependency: higher at higher treatment temperatures and lower at lower treatment temperatures. based on kinetic analysis, the apparent activation energy (E_a) was calculated as 407 kJ/mol, which is similar to the published E_a of lignin softening implying that the HTR is a lignin-related phenomenon.

Keywords

Compression wood, hygrothermal treatment, *Cryptomeria japonica*, activation energy, time-temperature superposition

Introduction

Steaming or boiling induces dimensional changes in green wood, which have been recognized as causing defects such as distortion, cracks, and the check of lumber during kiln drying at high temperature [1]. This dimensional change is called hygrothermal recovery (HTR) and is distinguished from other dimensional changes such as reversible thermal expansion, reversible expansion and contraction due to changes in moisture content, and irreversible expansion due to the breaking of hydrogen bonds [2–4]. According to a review by Kübler [1], the wood expands owing to HTR where the xylem generates compressive stress as residual elastic growth stress, while the wood contracts owing to HTR where the xylem generates tensional growth stress. The intensity of HTR also corresponds to the intensity of residual elastic growth stress.

The physical mechanism of HTR has been studied using reaction wood by examining the micro-morphological characteristics of xylem. The large contraction in the longitudinal (L) direction of tension wood due to HTR has a positive relationship with the ratio of gelatinous fiber or the gelatinous layer [5–7]. The expansion in the L direction of compression wood due to HTR has a significant relationship with a large microfibril angle [8], suggesting that HTR occurs in a mutual relationship between shrinkage of cellulose microfibrils and swelling of matrix substances in the wood cell wall, according to the reinforced-matrix theory [9].

Another important characteristic of HTR is time-temperature dependency, which is a physicochemical characteristic. Longer treatment duration or higher treatment temperature is known to cause larger dimensional changes [1]. Grzeczyński, Noack, and Sujan et al. observed the time-temperature dependency of HTR at temperature ranges of 40°C to 140°C, 100°C to 180°C, and 80°C to 120°C, respectively [10–12]. Based on these observations, HTR was estimated to be accelerated by increasing the temperature of treatment.

One possible interpretation of the HTR mechanism has been the long-term release of the viscoelastic component of residual growth stress that remains in the cell wall. Heating under the wet condition accelerates the release of the viscoelastic component of growth stress even after the elastic component is released immediately by cutting the xylem. Sasaki and Okuyama [13] modeled the distribution of residual growth stress based on the superposition theory of only the elastic component. By comparing it with measured elastic component and measured HTR, they demonstrated the effect of the viscoelastic component on growth stress. Gril and Thibaut [14] characterized HTR as an inverse phenomenon of generation of the viscoelastic component by rheological modeling. These studies suggested the presence of a viscoelastic component in the tree stem and the HTR was the product of residual growth stress. However, direct comparison between the elastic and viscoelastic components of growth stress has not been studied. Furthermore, if the viscoelastic component exists, the long-term behavior invoked by it at ambient conditions has not been investigated.

This study aimed to quantitatively investigate the relationship between HTR and the elastic growth stress as a factor or a quasi-factor of the HTR phenomenon. Specifically, the strain due to HTR was compared to the elastically released strain of standing trees by using compression wood and normal wood. This study also analyzed the time-temperature dependency and long-term behavior of HTR, not only to approach the physicochemical mechanism of HTR but also to simulate the possible behavior of HTR in living tree at ambient conditions.

Materials and Method

Sample trees

Five sugi (*Cryptomeria japonica*) trees that were 18–22 years old and grown in a research forest on Higashiyama campus of Nagoya University, Nagoya City, Japan, were used to measure growth stress and HTR (Table 1).

Measurement of released strain of surface growth stress

Released strain of elastic growth stress of the outermost surface of secondary xylem in longitudinal (L) direction (RS_L) and tangential (T) direction (RS_T) was measured based on established methods [15–17]. Four measuring points were set peripherally at five different heights of each standing tree (Fig. 1); in total, there were 100 measuring points for the five trees. Foil strain gauges made from polyimide, 10-mm-long (KFG-10-120-C1-11, Kyowa Electronic Instruments Co., Ltd.), were used and allowed a single-gauge three-wire connection. The gauges were glued with cyanoacrylate glue along the L and T directions and then connected to a handy strain meter (UCAM-1A, Kyowa Electronic Instruments Co., Ltd.). A groove in the secondary xylem surface around the gauge was carved out to 10 mm in depth using a handsaw to release surface growth stress. The released strains, RS_L and RS_T, were calculated as the difference between the initial strain and the strain with the groove.

Specimen preparation

Soon after harvesting, green specimens with the dimensions of approximately 30 mm (L) × 15 mm (T) × 5 mm (radial (R) direction) were cut from the same surfaces of the tree where the strain gauges were glued (Fig. 1), to determine the relationship between HTR and elastic growth stress. After removing the strain gauges from specimen surfaces, specimens were placed into 5 groups (no. 1−5) that showed similar histograms for RS_L. Specimens were kept wet throughout the preparation and the measurement of dimensions described below.

Measurement of Hygrothermal recovery

Longitudinal and tangential dimensions of green specimens, d_L^0 and d_T^0, respectively, were measured after conditioning at 20°C using digital comparators with reading accuracy of 0.001 mm (ID-S112, Mitutoyo Corporation). The digital comparators and rectangular gauge blocks as supporting boards were set on an iron surface plate so that all the specimens were at the same position for every measurement (Fig. 2). Two different positions were measured for each dimension of a specimen. After measuring d_L^0 and d_T^0, five groups of specimens with similar histograms for RS_L were subjected to hygrothermal treatment at five different temperatures with various treatment durations (Table 2). The specimens were heated in water at temperatures of 40, 60, 80, and 100°C, and were then immediately cooled in ice water and conditioned at 20°C overnight. The treatment at 20°C entailed keeping the specimens in water in a room at 20°C. After the treatment for each planned duration, dimensions (d_{L}^{t} and d_{T}^{t}) were carefully re-measured. Subsequently, the specimens were treated again. The cycle of hygrothermal treatment, cooling, and dimension measurement was repeated until the cumulative duration of treatment (t) was reached. The dimensional changes at t ($\varepsilon_{\mathrm{L}}^{t}$ and $\varepsilon_{\mathrm{T}}^{t}$) were calculated as follows:

$$\varepsilon_{\mathrm{L}}^{t} = 100\frac{d_{\mathrm{L}}^{t}-d_{\mathrm{L}}^{0}}{d_{\mathrm{L}}^{0}}\ (\%) \qquad (1)$$

$$\varepsilon_{\mathrm{T}}^{t} = 100\frac{d_{\mathrm{T}}^{t}-d_{\mathrm{T}}^{0}}{d_{\mathrm{T}}^{0}}\ (\%) \qquad (2)$$

The average values of two positions for each dimension were calculated for each specimen.

Results and Discussion

Released strain of growth stress

Table 3 shows the RS_{L} of all measuring points and the grouping of specimens so that all group members had similar histograms of RS_{L}. Trees with tilted stems showed more positive RS_{L} in the lower side of the stems. This result implies that a higher compressive growth stress was present in the lower side of the stems. Fig. 3 shows the negative correlation between RS_{L} and RS_{T}, which indicates the elastic two-dimensional deformation due to the release of growth stress.

General description of hygrothermal recovery

Typical changes at the 100°C treatment in $\varepsilon_{\mathrm{L}}^{t}$ and $\varepsilon_{\mathrm{T}}^{t}$ of specimens with various RS_{L} and RS_{T}, respectively, as functions of cumulative treatment duration t are shown in Fig. 4. The specimens with higher positive RS_{L} taken from compression wood expanded largely in the L direction after short-term treatment, while the specimens with negative RS_{L} from opposite wood showed minimal shrinkage in the L direction. In the T direction, the magnitude of $\varepsilon_{\mathrm{T}}^{t}$ was not related to RS_{T}. The relationship between $\varepsilon_{\mathrm{L}}^{t}$ and $\varepsilon_{\mathrm{T}}^{t}$ after treatment with planned maximum cumulative durations (20°C, t = 177 days; 40°C and 60°C, t = 24 days; 80°C and 100°C, t = 200 minutes) is shown in Fig. 5. In contrast to Fig. 3, plots in Fig. 5 did not show a clear relationship between $\varepsilon_{\mathrm{L}}^{t}$ and $\varepsilon_{\mathrm{T}}^{t}$, regardless of the values of RS_{L} and RS_{T}. The specimens taken from opposite wood with negative $\varepsilon_{\mathrm{L}}^{t}$ showed variable $\varepsilon_{\mathrm{T}}^{t}$ and the specimens from compression wood with higher positive $\varepsilon_{\mathrm{L}}^{t}$ generally showed positive $\varepsilon_{\mathrm{T}}^{t}$. These results suggest that the mechanism of HTR might not be explained as a simple deformation as for elastic release of growth stress.

As shown in Fig. 6, $\varepsilon_{\mathrm{L}}^{t}$ had a strong relationship with RS_{L}, while $\varepsilon_{\mathrm{T}}^{t}$ did not with RS_{T}. This result indicates that HTR in the L direction had a direct or indirect relationship with elastic growth stress, while HTR in the T direction was not related to the elastic growth stress or the effect of the elastic growth stress was masked by other factors. The intensity of HTR seemed to be temperature-dependent with both $\varepsilon_{\mathrm{L}}^{t}$ and $\varepsilon_{\mathrm{T}}^{t}$ being larger at higher treatment temperatures (Fig. 6). However, it is still premature to conclude that the intensity of HTR had temperature dependency because the $\varepsilon_{\mathrm{L}}^{t}$ and $\varepsilon_{\mathrm{T}}^{t}$ were still increasing at temperatures below 60°C.

Time and temperature dependency of hygrothermal recovery

Fig. 7a shows HTR behavior at each treatment temperature of the specimens that had similar values of RS_{L} (approximately 0.2% of RS_{L}, the values in framed boxes in Table 3). The increases of $\varepsilon_{\mathrm{L}}^{t}$ were more rapid during treatment at higher temperature than at lower temperatures. Although HTR has been considered to require a higher temperature than the softening points of wood constituents, mainly the lignin softening point of 70−100°C, the treatment at 40°C induced significant HTR of compression wood. No significant changes were observed at 20°C during the 177-day treatment. From the above results, it was clear that temperature strongly influenced the rate of HTR. At higher temperatures, the changes in $\varepsilon_{\mathrm{L}}^{t}$ were stronger. However, because $\varepsilon_{\mathrm{L}}^{t}$ seemed to still be increasing at 40°C and 60°C, the effect of temperature on the final values of $\varepsilon_{\mathrm{L}}^{t}$ are not clear. Temperature dependency should be considered in the rate of HTR but not in the final value of HTR.

Kinetic analysis of hygrothermal recovery

As already shown in Fig. 7a, the rate of HTR behavior depended on treatment temperature except for at 20°C. There are two possible explanations for HTR at 20°C: (1) HTR could occur but could not be observed within the range of t in this study; (2) HTR does not occur. However, growth stress was relaxed during long-term storage of logs even in ambient conditions whether under water or not [1]. Therefore, it would be interesting to consider the long-term effect of HTR, on the assumption that HTR occurs in ambient conditions. Thus, HTR was analyzed based on the kinetic approach for the quantitative investigation of temperature dependency.

The applicability of reaction kinetics such as zero, 1st, and 2nd order reactions was considered, as the determination of reaction formulae is a fundamental and important way to characterize unknown reactions. However, these reaction functions did not fit well to the HTR behavior observed in this study, especially to HTR below 60°C.

Therefore, the time-temperature superposition, a method to observe the whole procedure of the chemical reaction or mechanical behavior that has temperature dependency, was applied. Several studies in the fields of polymer and wood mechanics successfully used this approach to analyze the behavior of materials at various temperatures and to predict the behavior at the ambient temperature [18–24]. Although the ranges of temperature and duration in this study were limited, each curve of the isothermal changes in $\varepsilon_{\mathrm{L}}^{t}$ could be superposed to a single curve along with the time (log*t*) axis with proper shift distance for each temperature as shown in Fig. 7b. The data at 20°C were omitted since the changes in $\varepsilon_{\mathrm{L}}^{t}$ were not significant and shifting the data becomes meaningless. Proper shift distances that divided *t* to superpose each curve to a single curve were calculated for each treatment temperature (*T*), which is called shift factor (a_T) as follows:

$$\boldsymbol{a_T} = \frac{\boldsymbol{t_T}}{\boldsymbol{t_{ref}}} \qquad (3)$$

where t_{ref} is the treatment duration at the reference temperature T_{ref}. Referring to the previous instances [23–24], a logistic function with a constant was used to express a single curve to which all the plots were superposed;

$$f(x) = \frac{\alpha}{1+\beta\exp(-\gamma x)} + C \quad (4)$$

where $f(x)$ is the change in $\varepsilon_{\mathrm{L}}^{t}$, x is $\log(t_T/a_T)$, and α, β, γ, and C are constants. The temperature of 60°C was set as the arbitrary reference temperature, namely, $a_{T(=60°\mathrm{C})} = 1$. By using a_T, the apparent activation energy E_a can be determined based on the modified Arrhenius equation:

$$a_T = \exp\left[\frac{E_a}{R}\left(\frac{1}{T} - \frac{1}{T_{ref}}\right)\right] \quad (5)$$

where R is the gas constant (8.134 J $\mathrm{K^{-1}}$ $\mathrm{mol^{-1}}$). Plotting the natural logarithm of a_T versus the reciprocal of T as absolute temperature, called Arrhenius plot, is a way to calculate E_a.

Fig. 8 shows the Arrhenius plot with the values of ln a_T at each temperature. The Arrhenius plot showed the high linearity and the value of E_a calculated from the regression line of Arrhenius plot was 407 kJ/mol. Generally, the applicability of kinetics should be carefully considered when the temperature includes both below and over critical temperature of lignin [25–26]. Even though softening point of lignin in wet condition is around 70−100°C in both isolated and in situ lignin [25, 27–30], the Arrhenius plot did not deviate from the high linearity in the range from 40°C to 100°C. This showed that the Arrhenius approach could be applied to the HTR behavior in the temperature range of this study.

Prediction of hygrothermal recovery of compression wood during long-term life of tree

The values of $\varepsilon_{\mathrm{L}}^{t}$ at 20°C did not show obvious trend in the present experimental duration (177 days) as shown in Fig. 7a. However, if the Arrhenius plot could be extrapolated to the ambient temperature and HTR occurs at the ambient condition, xylem will change its dimensions during the long life of tree. Japanese cedar trees are harvested when the age of 60−100 years for commercial use and sometimes more than 100 years for special use such as traditional building, handcraft, and artworks. In certain area in Japan, the lifetime of Japanese cedar can exceed 1,000 years. It is suggestive for the mechanics of standing tree to estimate the dimensional change due to HTR that may possibly occur during long life of tree at the ambient conditions. Thus, the possible values of $\varepsilon_{\mathrm{L}}^{t}$ in compression wood at the ambient temperature during tree life were predicted. Two values of temperature, 20°C and 30°C, were set as the ambient temperature and then the values of $a_{T(=20°\mathrm{C})}$ and $a_{T(=30°\mathrm{C})}$ were calculated by extrapolating the regression line on the Arrhenius plot to these temperatures as shown in Fig. 8. The possible values of $\varepsilon_{\mathrm{L}}^{t}$ at t = 100 years and 1000 years were respectively determined by applying the calculated values of a_T to the formula (4): $\varepsilon_{\mathrm{L}}^{t}$ will be 0.035% and 0.15% during 100 years of tree life at 20°C and 30°C, respectively; 0.066% and 0.24% during 1,000 years at 20°C and 30°C, respectively. This rough estimation showed that HTR would induce not intense but significant dimensional change during realistic tree life of Japanese cedar growing in a temperate climate in Japan. While, since the measured values of $\varepsilon_{\mathrm{L}}^{t}$ for normal wood were considerably small, HTR of normal wood at the ambient temperature may not be significant.

General discussion about the origin of HTR

Based on the results described in the previous sections, here the origin of HTR was discussed from biomechanical and physicochemical viewpoints.

This study first compared the HTR ($\varepsilon_{\mathrm{L}}^{t}$) with the elastic component (RS_{L}) of growth stress and showed the intense relationship between $\varepsilon_{\mathrm{L}}^{t}$ and RS_{L}. This result indicated that the origin of HTR related to the generation of elastic component of growth stress, supposing $\varepsilon_{\mathrm{L}}^{t}$ represents the viscoelastic component of growth stress. During the maturation process of trees, growth stress is accumulated in their stems year by year, contributing the negative gravitropism of trees to support their huge body [31–33]. The growth stress has been discussed mainly in terms of only elastic dynamics. However, since the accumulation of elastic stress inevitably would accompany the accumulation of viscoelastic stress as well as elastic stress, previous reports suggested the presence of viscoelastic component of growth stress [13–14]. The intense relationship between $\varepsilon_{\mathrm{L}}^{t}$ and RS_{L} shown in this study practically supports the generation of viscoelastic components accompanying the generation of elastic component of growth stress during tree maturation.

The obtained value of E_a (407 kJ/mol) for compression wood is the other important characteristics to discuss the mechanism of HTR. The reported E_a values of the softening of *in situ* lignin in wet wood ranged from 240 to 440 kJ/mol depending on wood species [25, 30, 34]. Salmen reported the E_a values of 380 and 400 kJ/mol for Scandinavian pine (*Pinus silvestris*) and Norway spruce (*Picea abies*), respectively. Since these values were comparable to the value obtained from HTR in this study, HTR is possibly lignin-related behavior. Since the softening points of amorphous cellulose and hemicelluloses are under room temperature [27], they might not contribute to HTR. This implies that the thermal transition of lignin induced HTR, and that the higher amount of lignin in compression wood induced much more expansion in L direction as well as the higher microfibril angle in S2 layer relative to fiber axis of compression wood allows the expansion of the specimen in L direction, while the smaller expansion or contraction was induced in normal wood with the lower lignin content and the lower microfibril angle. From this viewpoint, HTR can be considered just a byproduct of the hygrothermal characteristics of lignin, and the intensity of HTR was controlled by the orientation of microfibril and the varying chemical composition to generate growth stress.

The possible mechanisms demonstrated in the above two paragraphs might be compatible or interact with each other. The authors, however, expects the further insights into the mechanism of HTR, which will be obtained by the precise measurement as well as morphological consideration such as the effort of cellulose microfibril.

Conclusion

The intensities of HTR in L and T directions were measured as dimensional changes by hygrothermal treatment in hot water at 20, 40, 60, 80, and 100°C to understand physicochemical characteristics of HTR and to compare the HTR with the elastic growth stress measured as the strain that is immediately released by cutting the xylem. The obtained results were as follows:

1) The rate of HTR showed time-temperature dependency: the HTR proceeded more rapidly at higher treatment temperature and more slowly at lower treatment

temperature. According to the kinetic analysis of the dimensional change in L direction for the compression wood specimens, the apparent activation energy was 407 kJ/mol, which was relevant to the energy of lignin softening in wet condition. This implied that HTR is the lignin-related phenomenon. The analysis also allowed simulating the long-term dimensional changes at the ambient temperature in living tree. The predicted dimensional changes during 100 years were 0.035% and 0.15% at the constant temperatures of 20°C and 30°C, respectively, in compression wood wherein large HTR was observed.

2) The HTR had a positive relationship with the elastic growth stress in L direction, and no relationship in T direction. The intense relationship between HTR and elastic growth stress in L direction practically supported the presence of the viscoelastic component of growth stress which is accumulated with the elastic component of growth stress during the tree maturation and is released by heating in wet conditions.

Acknowledgements

The authors are grateful to the member of Laboratory of Biomaterial Physics for their help to measure growth stress and harvest samples. The authors appreciate to Dr. Bertrand Marcon, Università degli Studi di Firenze, for providing a special set of devices combined to measure the dimensions.

Conflict of Interest

The authors have no conflict of interest directly relevant to the content of this article.

Reference

[1] Kübler H (1987) Growth stresses in trees and related wood properties, Forest Prod Abst 10:61–119.

[2] Yokota T and Tarkow H (1962) Changes in dimension on heating green wood, Forest Prod J 12:43–45.

[3] Sharma SN, Bali BI, Lohani RC (1978) Abnormal dimensional changes on heating green sal (*Shorea robusta*), Wood Sci 10:142–150.

[4] Bardet S, Gril J, Kojiro K (2012) Thermal strain of green Hinoki wood: separating the hygrothermal recovery and the reversible deformation. In: Frémond M and Maceri F (eds) Lecture notes in applied and computational mechanics, vol 61, mechanics, models and methods in civil engineering. Springer, Berlin, pp 157–162.

[5] Abe K and Yamamoto H (2007) The influences of boiling and drying treatment on

the behaviors of tension wood with gelatinous layers in *Zelkova serrata*, J Wood Sci 53:5–10.

[6] Clair B (2012) Evidence that release of internal stress contributes to drying strains of wood, Holzforschung 66:349–353.

[7] KC Sujan, Yamamoto H, Matsuo M, Yoshida M, Naito K, Shirai T (2015) Continuum contraction of tension wood fiber induced by repetitive hygrothermal treatment, Wood Sci Tech 49:1157–1169.

[8] Tanaka M, Yamamoto H, Kojima M, Yoshida M, Matsuo M, Abubakar ML, Hongo I, Arizono T (2014) The interrelation between microfibril angle (MFA) and hygrothermal recovery (HTR) in compression wood and normal wood of Sugi and Agathis, Holzforschung 68:823–830.

[9] Barber NF and Meylan BA (1964) The Anisotropic Shrinkage of Wood. A Theoretical Model, Holzforschung 18:146–156.

[10] Grzeczyński T (1962) Einfluß der Erwärmung im Wasser auf vorübergehende und bleibende Formänderungen frischen Rotbuchenholzes, Holz als Roh- und Werkstoff 20:210–216. [In German]

[11] Von D Noack (1969) About the hot-water treatment of European beech wood in the temperature range from 100 to 180°C, Holzforschung und Holzverwertung 21:118–124.

[12] Sujan KC, Yamamoto H, Matsuo M, Yoshida M, Naito K, Suzuki Y, Yamashita N, Yamaji FM (2016) Is hygrothermal recovery of tension wood temperature-dependent?, Wood Sci Tech, doi: 10.1007/s00226-016-0817-1.

[13] Sasaki Y and Okuyama T (1983) Residual stress and dimensional change on heating green wood, Mokuzai Gakkaishi 29:302–307.

[14] Gril J and Thibaut B (1994) Tree mechanics and wood mechanics: relating hygrothermal recovery of green wood to the maturation process, Ann Sci For 51:329–338.

[15] Okuyama T, Sasaki Y, Kikata Y, Kawai N (1981) The seasonal change in growth stress in the tree trunk, Mokuzai Gakkaishi 27: 350–355.

[16] Yamamoto H, Okuyama T, Iguchi M (1989) Measurement of growth stresses on the surface of a leaning stem, Mokuzai Gakkaishi 35:595–601. [In Japanese]

[17] Yoshida M and Okuyama T (2002) Techniques for measuring growth stress on the xylem surface using strain and dial gauges, Holzforschung 56:461–467.

[18] Ding HZ and Wang ZD (2007) Time-temperature superposition method for predicting the permanence of paper by extrapolating accelerated ageing data to ambient conditions, Cellulose 14:171–181.

[19] Gillen KT and Clough RL (1989) Time-temperature-dose rate superposition: A

methodology for extrapolating accelerated radiation aging data to low-dose rate conditions, Polym Degrad Stabil 24:137–168.

[20] Wise J, Gillen KT, Clough RL (1995) An ultrasensitive technique for testing the Arrhenius extrapolation assumption for thermally aged elastomers, Polym Degrad Stabil 49:403–418.

[21] Gillen KT and Celina M (2001) The wear-out approach for predicting the remaining lifetime of materials, Polym Degrad Stabil 71:15–30.

[22] Ding HZ and Wang ZD (2008) On the degradation evolution equations of cellulose, Cellulose 15:205–224.

[23] Matsuo M, Yokoyama M, Umemura K, et al (2011) Aging of wood: Analysis of color changes during natural aging and heat treatment, Holzforschung 65:361–368.

[24] Matsuo M, Umemura K, Kawai S (2014) Kinetic analysis of color changes in keyaki (*Zelkova serrata*) and sugi (*Cryptomeria japonica*) wood during heat treatment. J Wood Sci 60:12–20.

[25] Salmén L (1984) Viscoelastic properties of in situ lignin under water-saturated conditions. J Mater Sci 19:3090–3096.

[26] Nakano T (2012) Applicability condition of time-temperature superposition principle (TTSP) to a multi-phase system, Mech Time-Depend Mater 17:439–447.

[27] Goring DAI (1963) Thermal softening of lignin, hemicellulose and cellulose, Pulp and paper magazine of Canada, 64:T517– T527.

[28] Takamura N (1968) Studies on hot pressing and drying process in the production of fibreboard. III. Softening of fibre components in hot pressing of fibre mat, Mokuzai gakkaishi, 14:75–79.

[29] Hillis WE and Rozsa AN (1978) The softening temperature of wood, Holzforschung, 32:68–73.

[30] Furuta Y, Nakajima M, Nakanii E, Ohkoshi M (2010) The effects of lignin and hemicellulose on thermal-softening properties of water-swollen wood, Mokuzai gakkaishi, 56: 132–138 [in Japanese]

[31] Yamamoto H, Yoshida M, Okuyama T (2002) Growth stress controls negative gravitropism in woody plant stems, Planta 216:280–292.

[32] Fourcaud T and Lac P (2003) Numerical modelling of shape regulation and growth stresses in trees I. An incremental static finite element formulation, Trees 17:23–30.

[33] Fourcaud T, Blaise F, Lac P, et al (2003) Numerical modelling of shape regulation and growth stresses in trees II. Implementation in the AMAPpara software and simulation of tree growth, Trees 17:31–39.

[34] Olsson AM and Salmen L, (1992) Chapter 9 Viscoelasticity of in situ lignin as

affected by structure –softwood vs. hardwood. In: Glasser WG and Hatakeyama H (eds) ACS symposium series 489 Viscoelasticity of Biomaterials. ACS Publications, Washington, D.C. pp 133–143.

Tables

Table 1 Information about sample trees

Tree no.	Angle of tilt[a)] (°) Upper side/Lower side	Tree age (year)	DBH[b)] (cm)
1	13/13	18	10
2	14/13	19	13
3	15/14	19	8.9
4	6/2	22	8.9
5	5/3	22	13

a) Angle of tilt: angle between the uppermost or undermost side of the stem and the direction of gravitational force.

b) DBH: Diameter at breast height

Table 2 Treatment temperature and durations for each group.

Group no.	Temperature[a)] (°C)	Cumulative treatment duration (minute or day)
1	20	39, 42, 54, 89, 104, 127, 177 days
2	40	3, 6, 10, 20, 40, 100, 200, 400, 1000, 2440, 8860, 16240, 34780 minutes (= 24 days)
3	60	3, 6, 10, 20, 40, 100, 200, 400, 1000, 2440, 8860, 16240, 34780 minutes (= 24 days)
4	80	3, 6, 10, 15, 20, 40, 100, 200 minutes
5	100	3, 6, 10, 15, 20, 40, 100, 200 minutes

a) Treatment temperature of hygrothermal treatment

Table 3 Released strain of surface growth stress in longitudinal directions (RS_L) of each measured point. The values in framed boxes were RS_L of the specimens used for the kinetic analysis.

	Group 1	Group 2	Group 3	Group 4	Group 5
RS_L (%)	-0.033	-0.046	-0.035	-0.045	-0.048
	-0.032	-0.034	-0.034	-0.033	-0.046
	-0.028	-0.031	-0.028	-0.031	-0.028
	-0.027	-0.023	-0.028	-0.028	-0.025
	-0.024	-0.021	-0.027	-0.027	-0.025
	-0.021	-0.018	-0.023	-0.024	-0.015
	-0.014	-0.016	-0.022	-0.022	-0.013
	-0.012	-0.013	-0.019	-0.020	-0.013
	-0.001	-0.013	-0.018	-0.016	-0.011
	0.005	-0.011	-0.018	-0.010	-0.011
	0.005	-0.009	-0.008	-0.003	-0.007
	0.020	-0.002	0.013	0.001	0.013
	0.034	0.001	0.018	0.004	0.028
	0.055	0.029	0.042	0.022	0.033
	0.083	0.038	0.068	0.062	0.061
	0.130	0.063	0.094	0.071	0.066
	0.145	0.132	0.138	0.131	0.069
	0.171	0.155	0.167	**0.199**	0.118
	0.220	**0.196**	**0.207**	0.211	0.178
	0.284	0.232		0.254	**0.214**

Figure captions

Fig. 1 Positions where the released strain of surface growth stress were measured by strain gauges and where specimens were taken.

Fig. 2 Measurement of longitudinal and tangential dimensions of the specimens. Gauge blocks to support specimens and digital comparators were fixed by strong magnets on an iron surface plate.

Fig. 3 Relationship between released strain of tangential growth stress (RS_{T}) and that of longitudinal growth stress (RS_{L}).

Fig. 4 Dimensional changes in L and T directions ($\boldsymbol{\varepsilon}_{\mathbf{L}}^{\boldsymbol{t}}$ and $\boldsymbol{\varepsilon}_{\mathbf{T}}^{\boldsymbol{t}}$) as functions of cumulative treatment duration (t): several typical examples at 100°C treatment and of the compression wood and the opposite wood with their released strain of growth stress (RS_{L} and RS_{T}). Compression wood showed higher values of RS_{L} and lower values of RS_{T} and normal wood showed lower RS_{L} and higher RS_{T}.

Fig. 5 Relationship between dimensional changes in L direction ($\boldsymbol{\varepsilon}_{\mathbf{L}}^{\boldsymbol{t}}$) and those in T direction ($\boldsymbol{\varepsilon}_{\mathbf{T}}^{\boldsymbol{t}}$) after the treatment of the maximum cumulative durations.

Fig. 6 Relationship between dimensional changes ($\boldsymbol{\varepsilon}_{\mathbf{L}}^{\boldsymbol{t}}$ or $\boldsymbol{\varepsilon}_{\mathbf{T}}^{\boldsymbol{t}}$) after the treatment of maximum cumulative durations and released strain of growth stress (RS_{L} or RS_{T}).

Fig. 7 a) Typical change in longitudinal dimensions during hygrothermal treatment of the specimens that have approximately 0.2% of released strain (RS_{L}). (20°C: 0.220%, 40°C: 0.196%, 60°C: 0.207%, 80°C: 0.199%, 100°C: 0.214%). b) Data superposed to a single curve by the appropriate values of shift factors (a_T).

Fig. 8 Arrhenius plot derived from time-temperature superposition of HTR (Fig. 7) with shift factors (a_T) of each temperature (T). The calculated value of apparent activation energy (E_a) was 407kJ/mol. a) The values at 20°C and 30°C were calculated by extrapolating the regression line on the Arrhenius plot to each temperature.

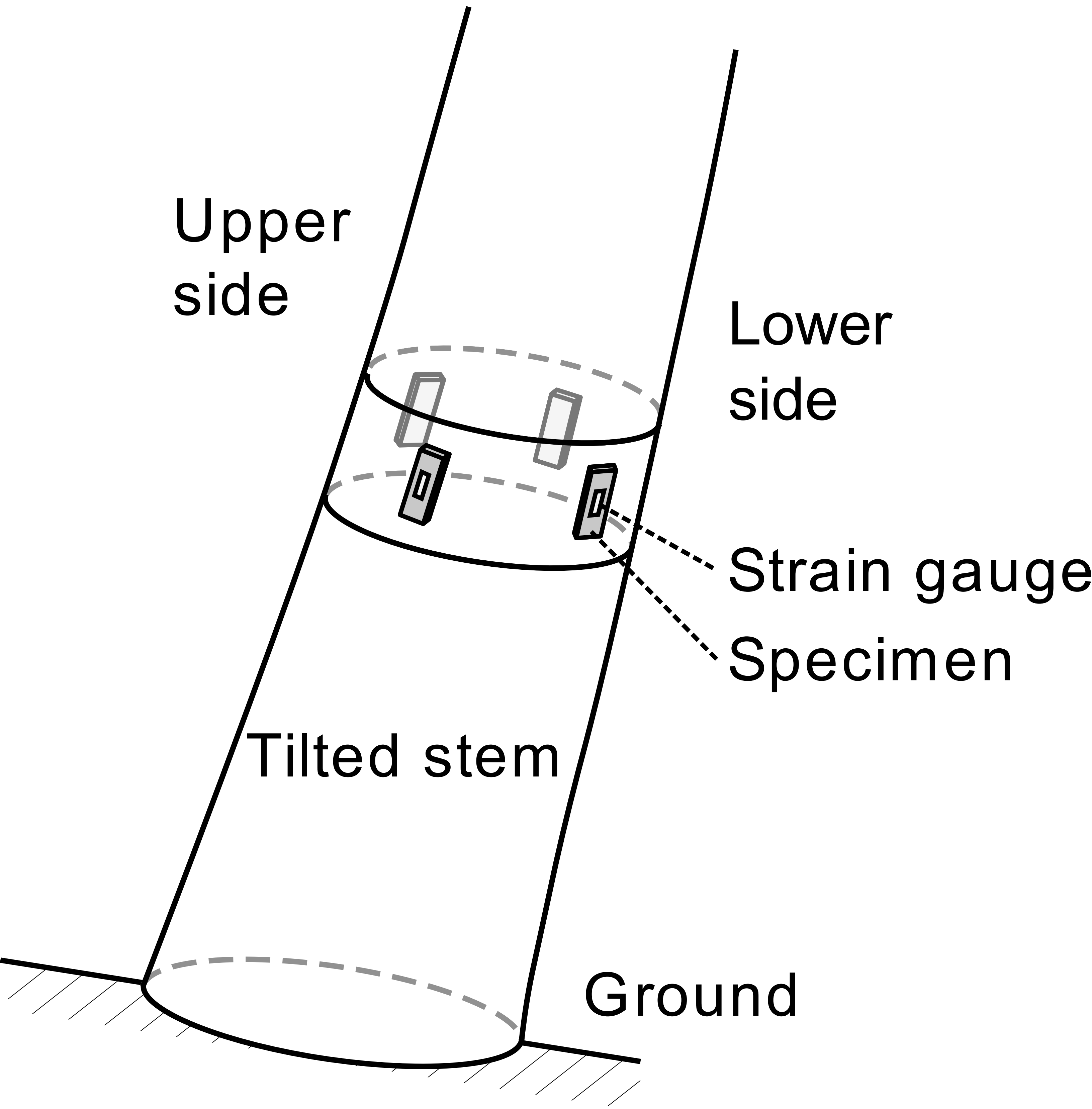
Upper side
Lower side
Strain gauge
Specimen
Tilted stem
Ground

Fig2

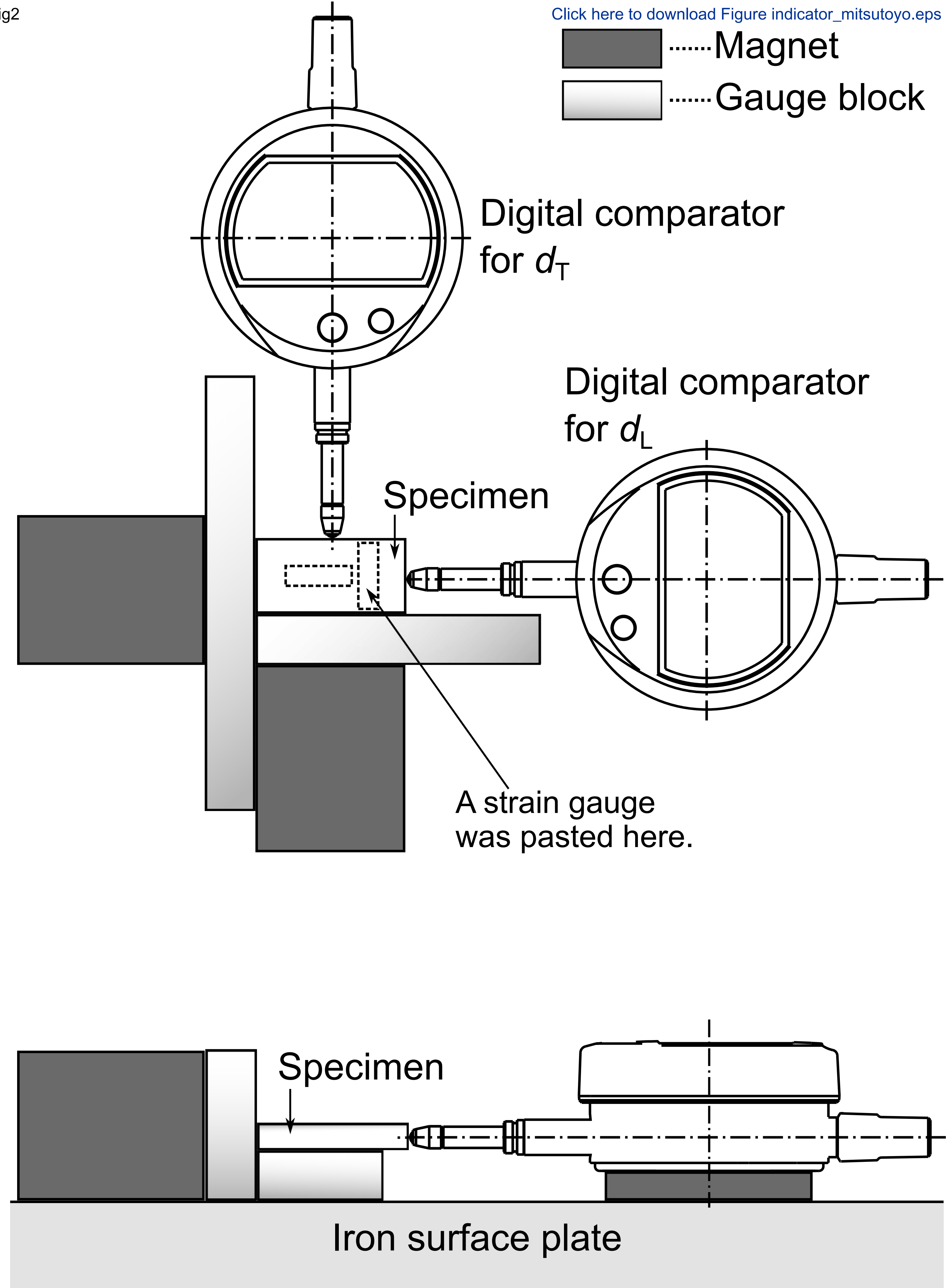
Magnet
Gauge block
Digital comparator for d_T
Digital comparator for d_L
Specimen
A strain gauge was pasted here.
Specimen
Iron surface plate

Fig3

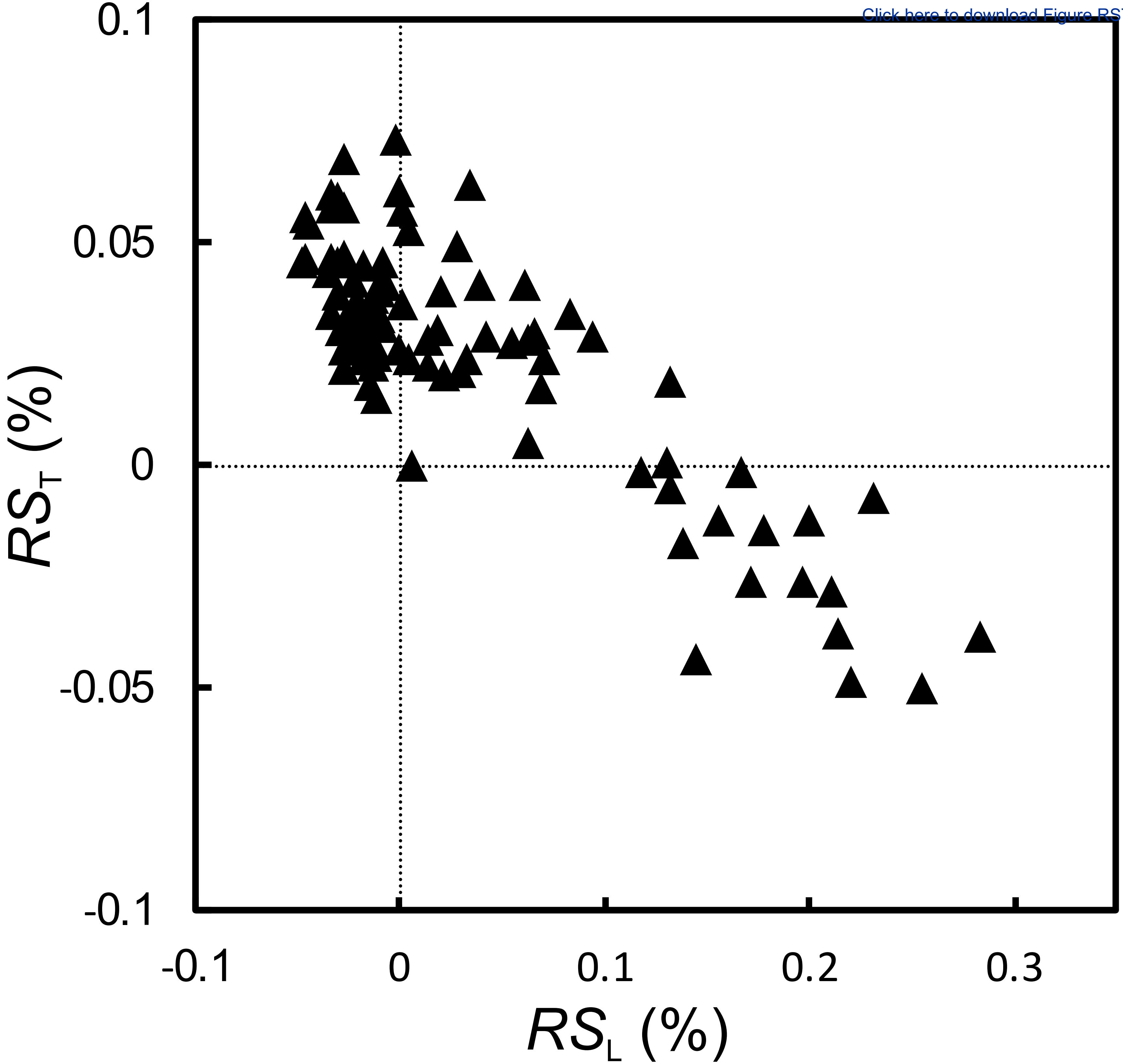

Fig4

Click here to download Figure trend.eps

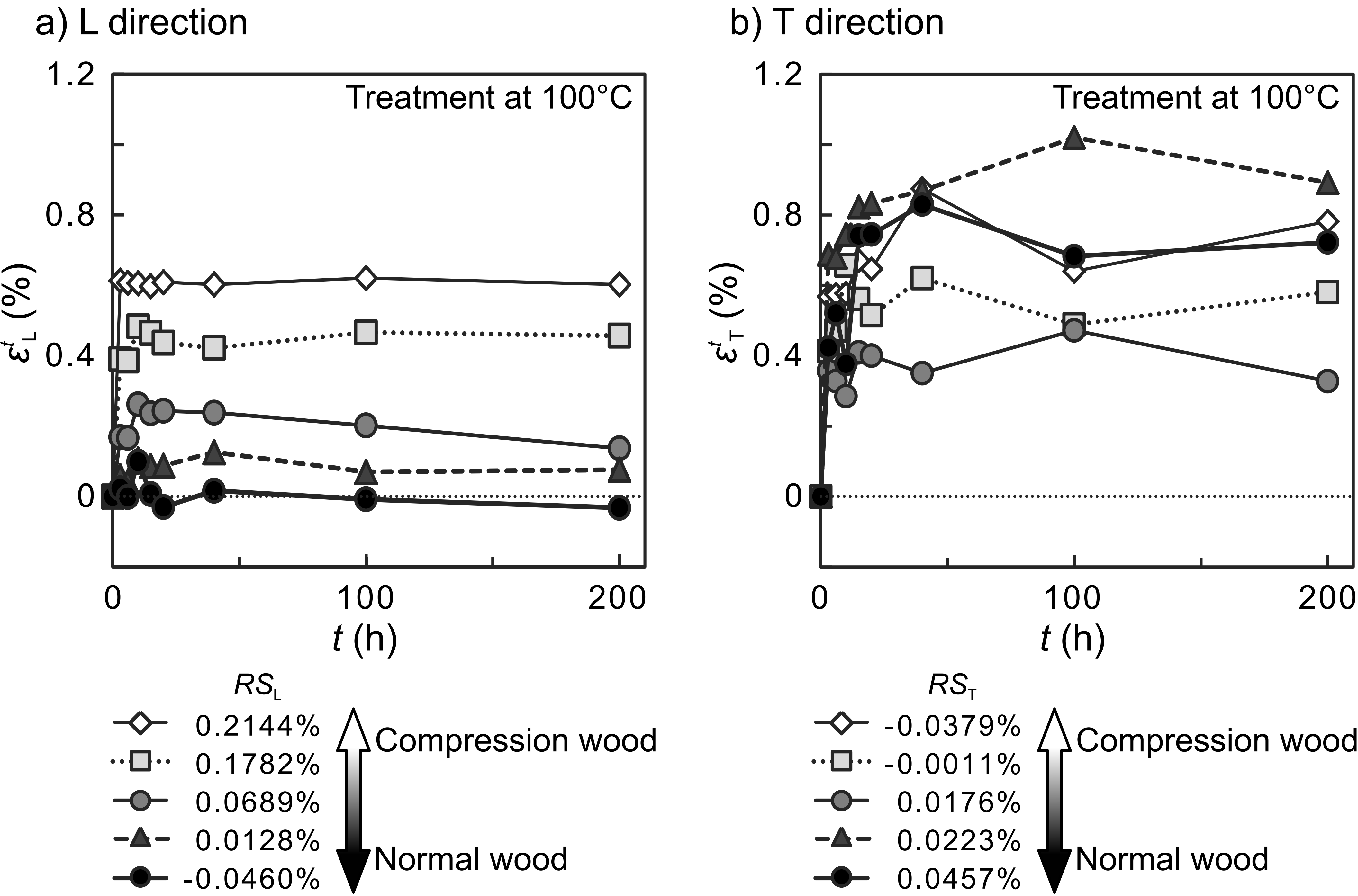

Fig5

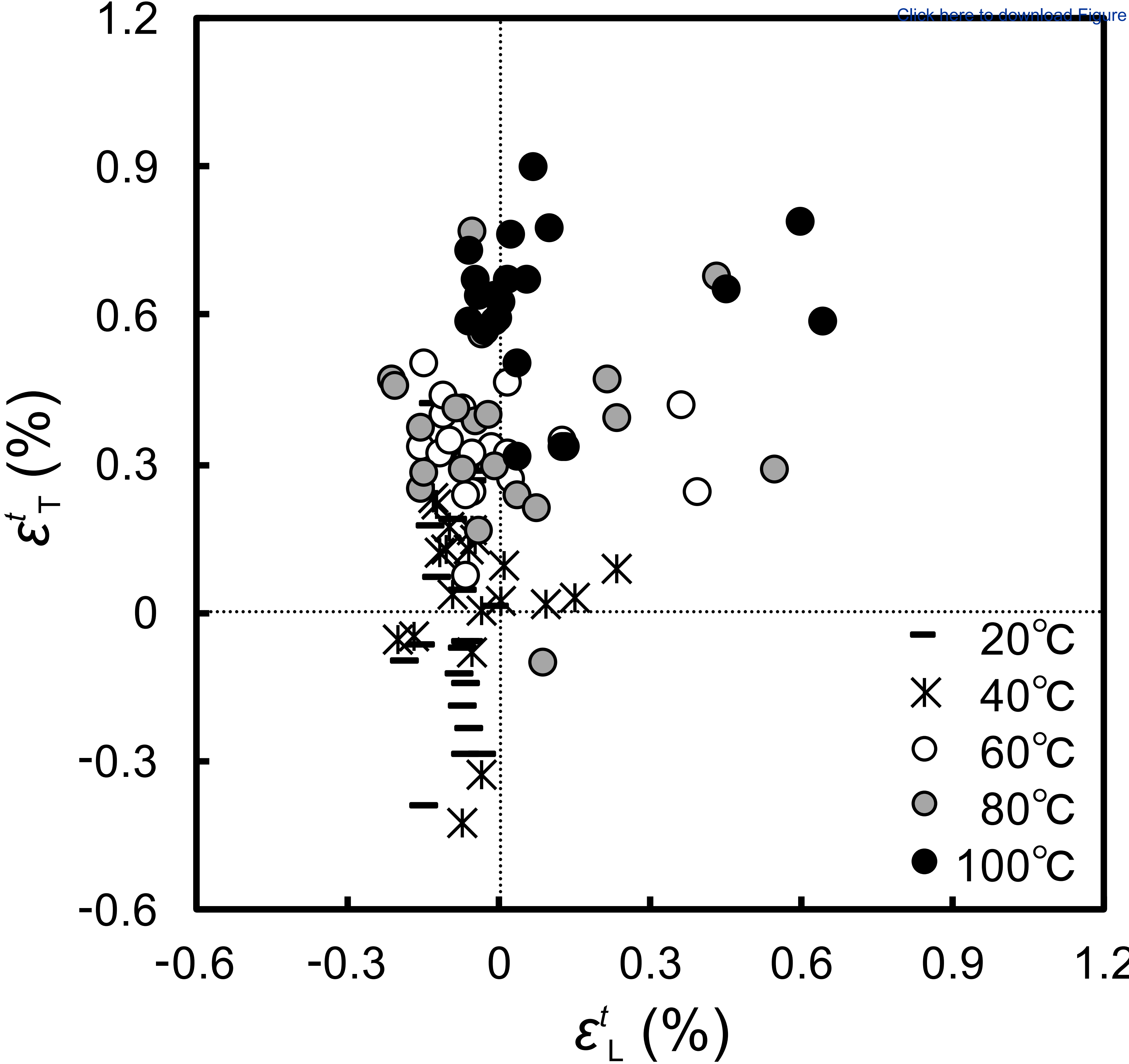
1.2
0.9
0.6
0.3
0
-0.3
-0.6
ε^t_T (%)
-0.6
-0.3
0
0.3
0.6
0.9
1.2
ε^t_L (%)
20°C
40°C
60°C
80°C
100°C

Fig6

Click here to download Figure dvsRS.eps

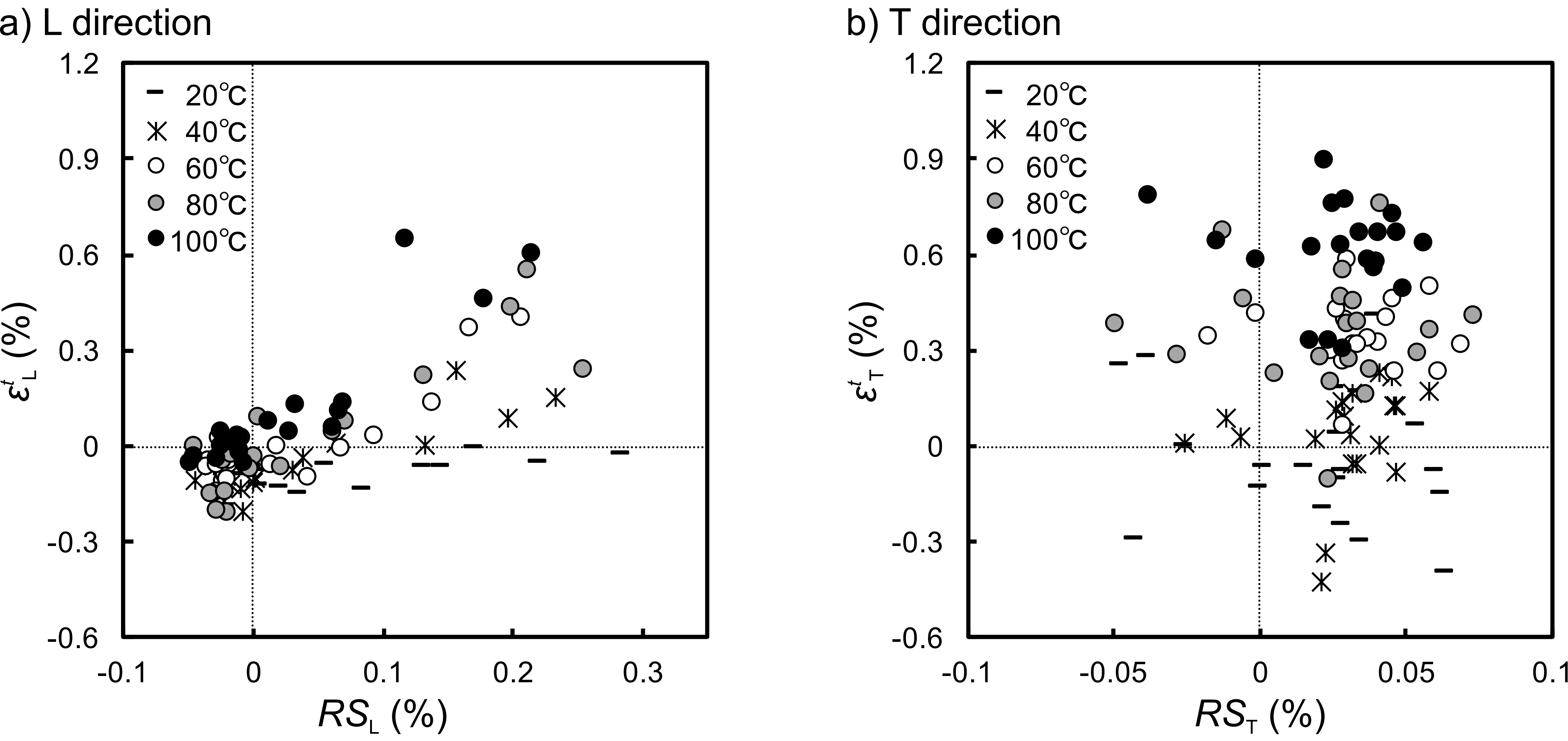

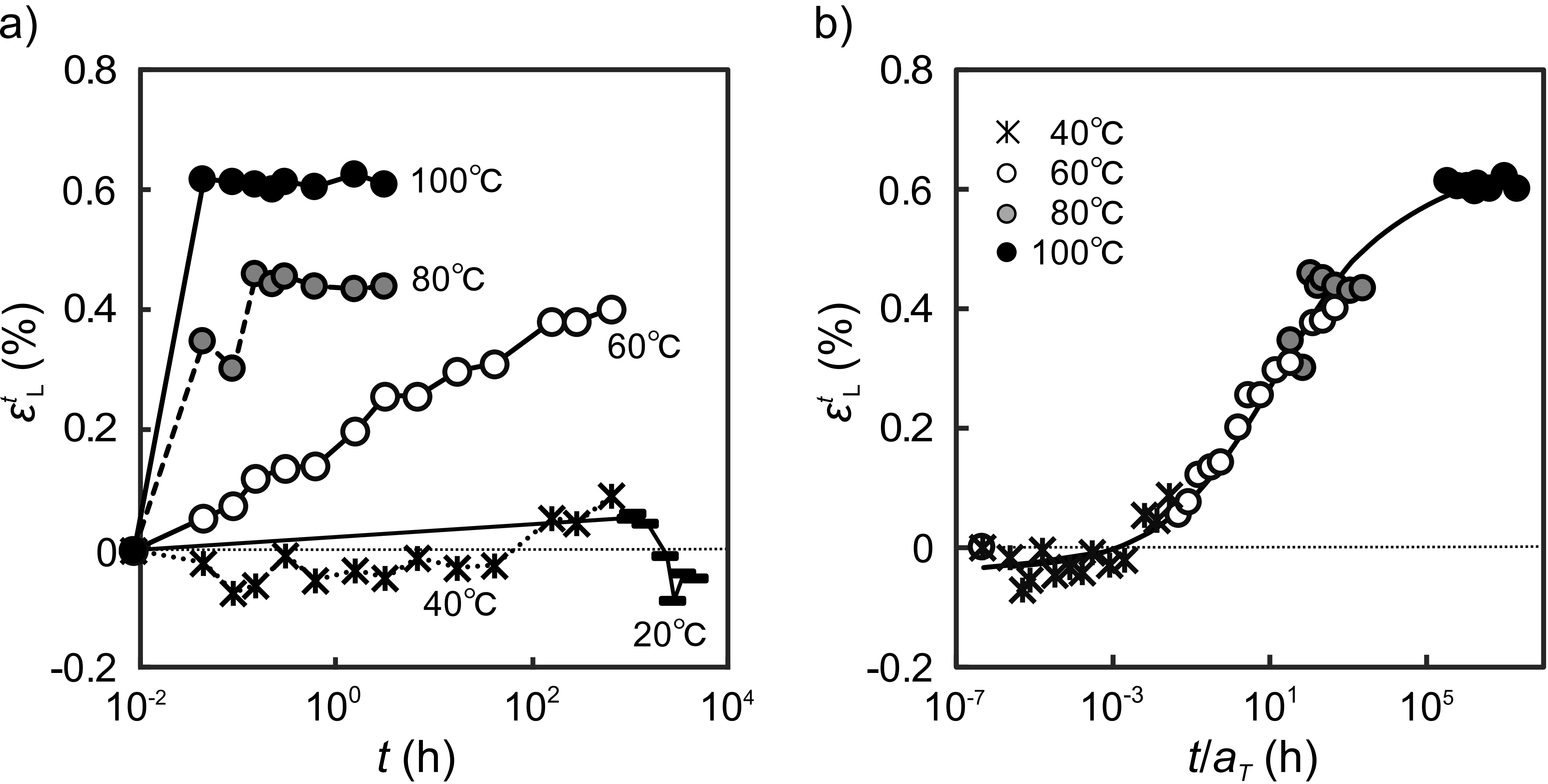
a)
0.8
0.6
0.4
0.2
0
-0.2
ε^t_L (%)
100°C
80°C
60°C
40°C
20°C
10^{-2}
10^0
10^2
10^4
t (h)
b)
0.8
0.6
0.4
0.2
0
-0.2
ε^t_L (%)
40°C
60°C
80°C
100°C
10^{-7}
10^{-3}
10^1
10^5
t/a_T (h)

Fig8

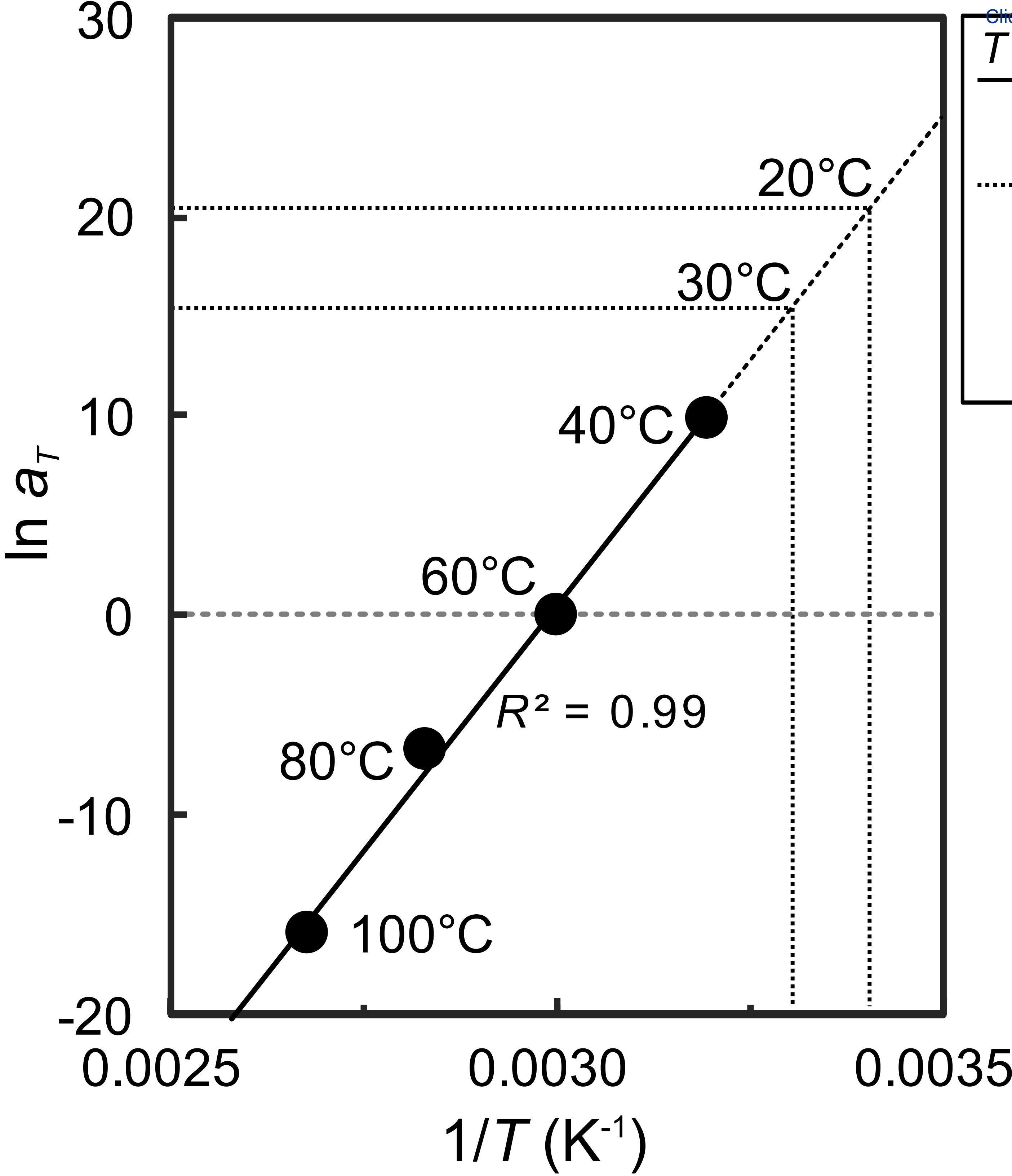

T (°C)	ln a_T
20	20.6*
30	15.1*
40	9.92
60	0
80	-6.63
100	-15.8